Volume 4 | Number 2 | 14 January 2016 | Pages 331–686

Journal of Materials Chemistry A

Materials for energy and sustainability

www.rsc.org/MaterialsA

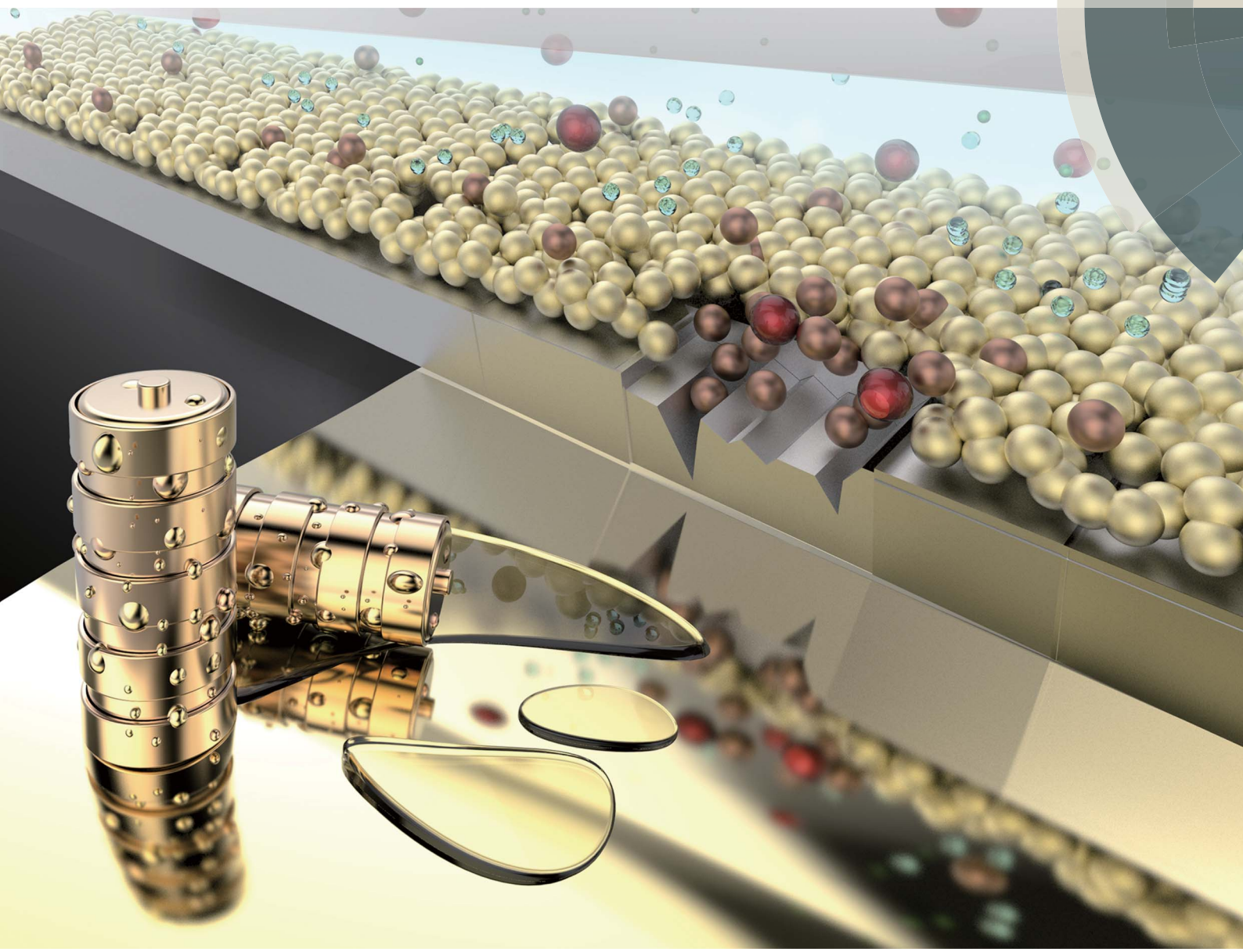

ISSN 2050-7488

ROYAL SOCIETY OF CHEMISTRY

PAPER

Yan Yao *et al.*

Chromate conversion coated aluminium as a light-weight and corrosion-resistant current collector for aqueous lithium-ion batteries

175 YEARS

Journal of Materials Chemistry A

PAPER

View Article Online
View Journal | View Issue

Cite this: J. Mater. Chem. A, 2016, 4, 395

Chromate conversion coated aluminium as a light-weight and corrosion-resistant current collector for aqueous lithium-ion batteries

Saman Gheytani,[a] Yanliang Liang,[a] Yan Jing,[a] Jeff Q. Xu[b] and Yan Yao*[ac]

Received 14th September 2015
Accepted 15th October 2015

DOI: 10.1039/c5ta07366a

www.rsc.org/MaterialsA

Aqueous batteries constructed using non-flammable water-based electrolytes have the potential to improve the safety and reduce the cost of energy storage to enable mass adoption of electric vehicles. The use of low-cost and lightweight aluminium foil as a current collector in aqueous batteries is tempting but also challenging due to corrosion reactions. Here we report chromate conversion coated (CCC) aluminium foil as a corrosion-resistant current collector in aqueous lithium-ion battery cathodes. CCC aluminium-based electrodes show better cycling stability and higher coulombic efficiency than those fabricated on stainless steel and titanium foils. Furthermore, CCC aluminium foil suppresses oxygen evolution at high potentials. The plausibility of using such lightweight corrosion-resistant current collectors for aqueous batteries marks an important step toward low-cost, high-energy, and safe energy storage.

1. Introduction

Aqueous lithium-ion batteries (ALIBs) combining the 'rocking-chair' principle of conventional LIBs and the use of low-cost, non-flammable water-based electrolytes are more promising technologies than organic electrolyte-based lithium-ion batteries (LIBs) in terms of safety, flexibility in electric vehicle design, and system cost reduction.[1,2] The aggressive nature of the aqueous environment increases the necessity for electrochemically stable components of the ALIBs including electrode and current collector materials.[3] In the past two decades, much progress has been made towards developing stable cathode and anode materials compatible with aqueous electrolytes.[4] In contrast, less study has been performed focusing on the development of current collectors. To date, only well-known corrosion-resistant materials such as titanium,[5] stainless steel (SS),[6] nickel,[7] and platinum[8] have been used as current collectors in ALIB studies. Table 1 compares the price and areal weight of these materials alongside aluminium which is the well-established current collector in conventional non-aqueous LIBs.[9] Aluminium appears to be the best candidate because light-weight and low-cost materials as current collectors are critical for enabling viable and practical applications.[9] However, aluminium is prone to corrosion in aqueous environments,[10] especially under an applied potential when reaction and ionic migration are accelerated.[11] Many methods have been developed in the past to prevent aluminium corrosion based on isolating the surface with a barrier coating to suppress the cathodic reaction of corrosion by limiting the diffusion of the electrolyte to the surface.[12]

Among various organic and inorganic coatings, chromium compound based films are currently the most effective way to inhibit corrosion of aluminium and its alloys. Chromate conversion coating has also been identified as a simple, cheap, and fast method to passivate the aluminium surface with a thin and impervious layer of chromium oxide and related Cr(III) compounds.[13] Here we report the successful use of chromate conversion coated (CCC) aluminium foil as a light-weight and corrosion-resistant current collector for use in ALIBs. Our results showed that the overall performance of the $LiMn_2O_4$ electrodes on CCC aluminium current collectors is superior to

Table 1 Comparison of price and areal weight of various materials used as collectors in commercial batteries[a]

Current collector	Price ($ per ft^2)	Weight (g per ft^2)	Resistivity (Ω m) at 293 K
Stainless steel (SS316)	19	92	6.9×10^{-7}
Nickel	31	105	6.9×10^{-8}
Titanium	109	53	4.2×10^{-7}
Aluminium	0.6	31	2.82×10^{-8}

[a] Price information calculated based on foils with the same thickness (0.2 mm). Data obtained from http://www.McMaster.com in April 2015.

[a]Department of Electrical and Computer Engineering, Materials Science and Engineering Program, University of Houston, Houston, Texas 77204, USA. E-mail: yyao4@uh.edu

[b]Southwest Research Institute, 6220 Culebra Road, San Antonio, Texas 78228-0510, USA

[c]Texas Center for Superconductivity, University of Houston, Houston, Texas 77204, USA

those of electrodes fabricated on more expensive and heavier materials in terms of cyclability and coulombic efficiency, thereby introducing new opportunities for the development of low-cost, stable, and high efficiency current collectors for aqueous batteries.

2. Experimental section

2.1. Chromate conversion coating of aluminium foil

CCC aluminium foil was fabricated by a "MIL-C-5541E Class 3" process.[14] This process consists of the following steps: (a) pre-treatment of the aluminium foil surface by a deoxidizer (Oakite 160) solution with intermittent water rinsing, (b) immersing aluminium foil in a chromic acid solution (CrO_3 3.7 g l^{-1}, NaF 1.2 g l^{-1}, and $Na_2Cr_2O_7$ g l^{-1}, pH = 1.8) for 120 seconds, (c) rinsing with water at 45 °C, and (d) drying in air at 50–60 °C. This process produces an extremely corrosion-resistant film composed of hydrated mixed Cr(III) and Al(III) oxides:[15]

$$2Al + Cr_2O_7^{2-} + 2H^+ + H_2O \rightarrow 2CrOOH\downarrow + 2AlOOH\downarrow \quad (1)$$

The AlOOH in the mixed oxides is then dissolved due to the fluoride ions present in the coating solution, leaving the less soluble CrOOH in the coating. This process continues as the strongly adhered coating grows to clog the aluminium surface with the bulk coating consisting of Cr_2O_3 and CrOOH.[15] The coating was characterized with X-ray photoelectron spectroscopy (XPS, Physical Electronics Model 5700) and scanning electron microscopy (SEM, Gemini LEO 1525 microscopy).

2.2. Electrode fabrication

For titanium, un-treated aluminium, and CCC aluminium foil current collectors, the working electrodes were prepared by spreading a slurry of commercial $LiMn_2O_4$ powder (purchased from MTI, particle size distribution 10–20 μm), carbon black (TIMCAL), and polyvinylidene difluoride (weight ratio 80 : 10 : 10) in *N*-methyl pyrrolidinone on the substrate followed by drying. For the SS mesh substrate, the electrodes were made by using polytetrafluoroethylene as the binder. The surface area of each electrode was 1.5 cm^2.

2.3. Electrochemical measurements

All the electrochemical characterizations were conducted in a three-electrode flooded-cell configuration using fabricated $LiMn_2O_4$ electrodes as the working electrode, activated carbon as the counter electrode, and Ag/AgCl as the reference electrode immersed in 5 ml of 2.5 M Li_2SO_4 as the electrolyte. All electrochemical measurements including constant current charging–discharging, voltammetry measurements, and electrochemical impedance spectroscopy (EIS) were carried out using a Biologic VMP3 potentiostat.

3. Results and discussion

Fig. 1 compares the morphology and XPS spectra of the aluminium surface before and after CCC treatment. Fig. 1(a) and (b) show the surface morphology of un-treated and CCC aluminium foils, respectively. The un-treated aluminium foil surface has parallel streaks and small micro-indentations resulting from mechanical rolling operations. In contrast, CCC aluminium foil shows a uniform mud-crack pattern (Fig. 1(b)). Dehydration of the CCC film develops tensile stress leading to the formation of cracks, in particular during drying of the coating and is characteristic of the CCC layer.[16] Absence of peel-off spots over the surface can be interpreted as the good coverage and adhesion of the coating.[17] The XPS Al 2p spectra of the un-treated and CCC aluminium foils are shown in Fig. 1(c). The Al 2p signals appearing at 75.8 eV and 72.9 eV for the un-treated aluminium foil are characteristic of aluminium oxide and aluminium metal, respectively. Neither of the peaks are detected after the CCC process, indicating complete coverage of the aluminium surface.[18] Fig. 1(d) shows the XPS spectra of Cr $2p_{3/2}$, where the peaks at 579.5 eV and 581.3 eV indicate the presence of Cr(III) as in CrOOH and Cr(VI) as in chromate, respectively.[19] The presence of chromate in the coating is believed to contribute to the "active corrosion inhibition" upon any corrosive attack to the surface (*vide infra*).[20]

In order to show the improvement of the performance of aluminium foil after the CCC process, the electrochemical performance of $LiMn_2O_4$ electrodes fabricated on both un-treated and CCC aluminium foils as the current collectors is presented in Fig. 2. The electrode fabricated on un-treated aluminium foil suffers from large capacity loss each cycle. The black spots on the backside of the aluminium foil after 15 cycles are the formed corrosion pits (inset in Fig. 2(a)). In contrast, 86% of the specific discharge capacity of the electrode fabricated on CCC aluminium foil retained after 50 cycles with the characteristic two-plateau potential profile of $LiMn_2O_4$ preserved (Fig. 2(b)).[21] The absence of black spots in the inset of

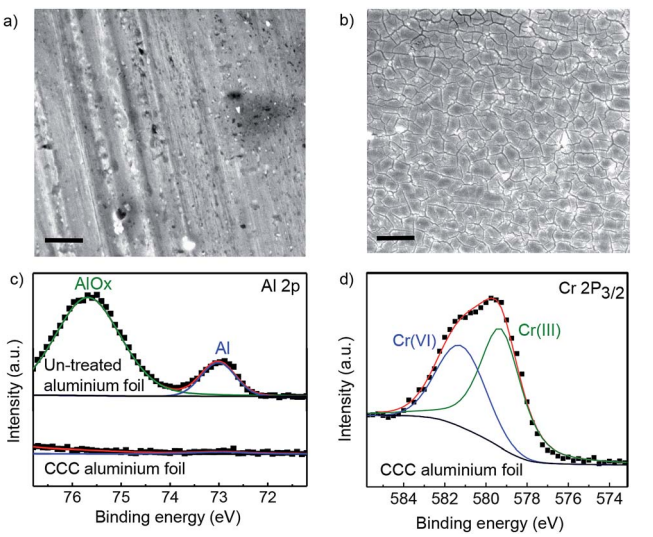

Fig. 1 Characterization of CCC aluminium foil. SEM image of the surface obtained from aluminium foil (a) before and (b) after coating (scale bar: 10 μm). (c) XPS Al 2p spectra of aluminium foil before and after coating; and (d) XPS Cr $2p_{3/2}$ for CCC aluminium foil.

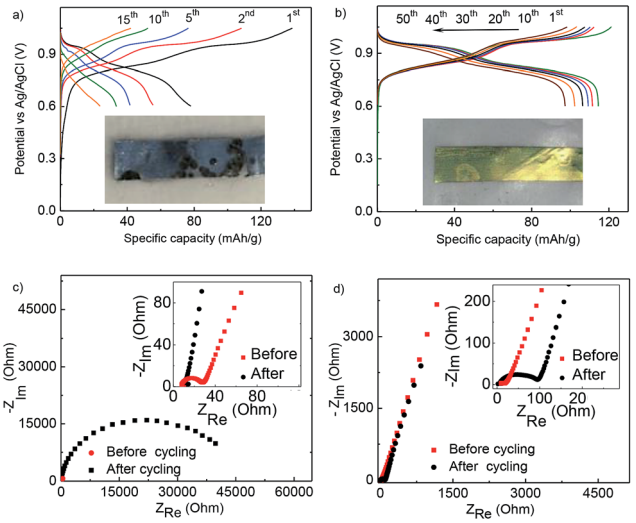

Fig. 2 Electrochemical characterization of $LiMn_2O_4$ electrodes on un-treated aluminium and CCC aluminium foil as current collectors. (a) Charge–discharge voltage curve of different cycles in 2.5 M Li_2SO_4 electrolyte (pH = 7) for the $LiMn_2O_4$ electrode on un-treated aluminium foil. The inset shows the photograph of the backside of the un-treated aluminium foil current collector after 15 cycles. (b) $LiMn_2O_4$ electrode on CCC aluminium foil. The inset shows the photograph of the backside of the CCC aluminium foil current collector after 50 cycles. The golden color is the typical color of CCC coating. Impedance spectra for (c) un-treated aluminium foil and (d) CCC aluminium foil before and after cycling. In both (c) and (d), the insets show the magnified high frequency region.

Fig. 2(b) confirms the inhibition of corrosion during cycling. The golden color is typical for CCC coating.

Impedance spectra of the electrodes were analysed for both un-treated and CCC aluminium foil electrodes to reveal the property change of the current collectors before and after cycling. According to the simplified contact-Randles (SCR) equivalent circuit proposed for impedance spectra of lithium-ion insertion electrodes by Atebamba *et al.*,[22] the EIS spectrum was composed of two partially overlapped arcs in the high to medium frequencies. The high-frequency arc is attributed to the impedance due to the collector-electrode materials contact. At medium-frequency, there is another arc due to charge transfer resistance between active materials and the electrolyte. The electrochemical impedance can be estimated from the diameter of the arcs from the impedance spectra.[23] Fig. 2(c) shows the increase of the combined impedance from 30 to 45 000 Ω after only 15 cycles. This dramatic increase is due to the continuous corrosion of the un-treated aluminium current collector. In contrast, for the CCC electrode, there is only a relatively small increase from 30 to 100 Ω after 50 cycles (Fig. 2(d)).

In the aluminium–water system, pitting corrosion is the most common type of corrosion at room temperature and starts as soon as aluminium is exposed to the aqueous environment. During charging, the corrosion is accelerated due to anodic polarization.[20]

Fig. 3(a)–(c) show the corrosion process of un-treated aluminium. In the first stage (Fig. 3(a)), pitting is initiated by the aggressive ions (*e.g.* sulfate) in the solution that penetrate the passivation film.[24] The corrosion of aluminium occurs in two steps (Fig. 3(b)):

$$Al \rightarrow Al^{3+} + 3e^- \quad (2)$$

$$Al^{3+} + 3H_2O \rightarrow Al(OH)_3 + 3H^+ \quad (3)$$

Aluminium is first oxidized, and the resulting aluminium ions react with water to form $Al(OH)_3$ precipitates and decrease the pH inside the pit. To balance the positive charge, more sulfate ions migrate into the pits which propagate the pitting (Fig. 3(c)). Meanwhile, the electrons stripped from aluminium are captured at the passivated aluminium surface by the cathodic reduction of water:[10]

$$2H_2O + 2e^- \rightarrow H_2 + 2OH^- \quad (4)$$

Local alkalinization at the cathodic sites results in dissolution of the passivation film and formation of new corrosion sites.[25]

The CCC aluminium, on the other hand, has a Cr(III) surface film that acts as an impervious physical barrier to the corrosive aqueous electrolyte.[26] Even though with cracks (as observed with SEM), the CCC coating has the ability of self-healing *via* an

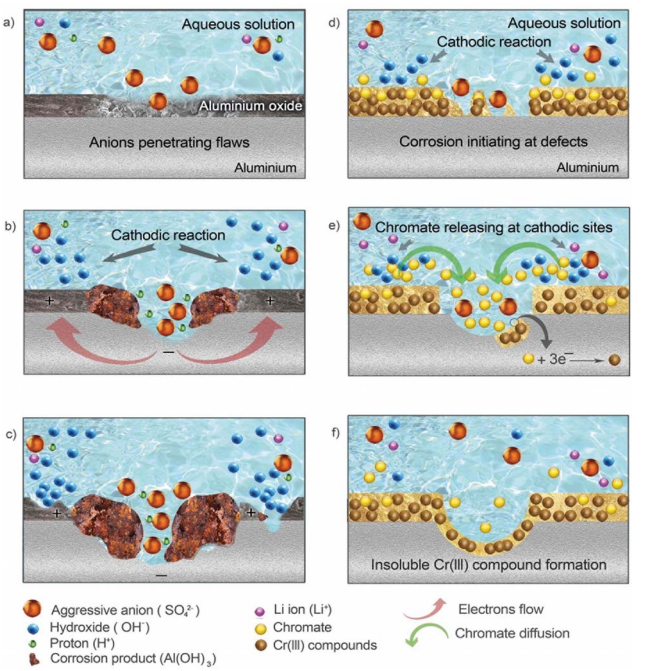

Fig. 3 Schematics of the corrosion behavior of un-treated (a–c) and CCC (d–f) aluminium in aqueous electrolytes. (a) Pitting initiation, (b) propagation of the pit and formation of $Al(OH)_3$ as the corrosion product, and (c) local increase of pH around the pit and formation of new corrosion sites. (d) Initiation of a corrosion site at an un-protected site on the surface, (e) chromate released to the solution as a result of pH increase around the corrosion site followed by chromate reduction to form insoluble Cr(III) compounds, and (f) passivation of the corrosion site as insoluble Cr(III) formed.

"active corrosion inhibition" process aided by the stored chromate in the coating layer:[27]

$$OCr(III)–O–Cr(VI)O_3^- + OH^- \Leftrightarrow CrOOH + CrO_4^{2-} \quad (5)$$

$$CrO_4^{2-} + 3H_2O + 3e^- \rightarrow CrOOH + 5OH^- \quad (6)$$

where CrOOH is representative of hydrated Cr(III) oxides. Chromate ions originally adsorbed on Cr(III) through a reversible Cr(VI)–O–Cr(III) bond can be favorably released at higher pH values near the cathodic sites (Fig. 3(d) and (e)).[27,28] The chromate ions readily diffuse to the corrosion sites, where they are reduced and form insoluble Cr(III) compounds as shown in Fig. 3(e). Therefore, the combination of storage, release, migration, and irreversible reduction of chromate enables efficient protection of aluminium at the cracked sites (Fig. 3(f)).

To demonstrate the competitiveness of CCC aluminium as a current collector material for ALIBs *vis-à-vis* state-of-the-art materials, the galvanostatic charge–discharge performance for $LiMn_2O_4$ electrodes fabricated on a series of current collectors including CCC aluminium, untreated aluminium, SS316 mesh, and titanium foil is compared in Fig. 4. Fig. 4(a) reveals that the lowest electrode polarization was obtained with the electrode on CCC aluminium foil. Compared to the $LiMn_2O_4$ electrode fabricated on titanium and SS, the electrode on CCC aluminium foil is superior in terms of stability with an 86% capacity retention after the first 50 cycles (Fig. 4(b)). For comparison, the electrode on un-treated aluminium foil delivered almost no capacity after 25 cycles. Note that the capacity decay for all the electrodes is related to the intrinsic instability of the micron-sized $LiMn_2O_4$ particles due to Jahn–Teller distortion and Mn dissolution during cycling.[29] Reduction of the particle size to the nanoscale can help mitigate the instability of $LiMn_2O_4$ but is beyond the scope of this work.[30]

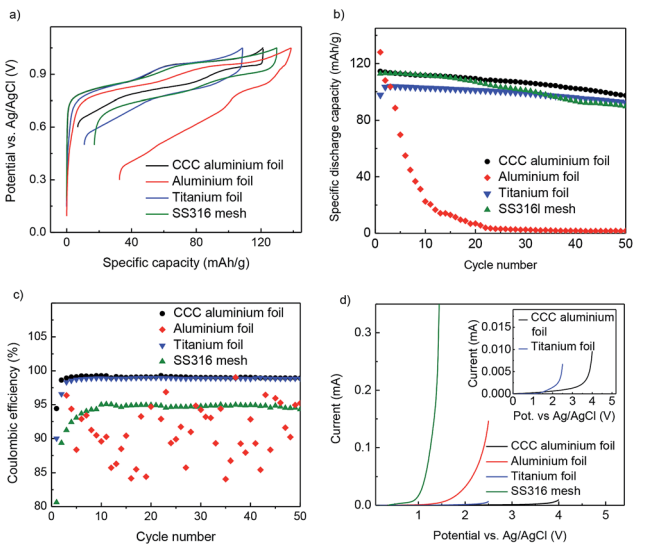

Fig. 4 Comparison of electrochemical performance of $LiMn_2O_4$ electrodes fabricated on different current collectors in 2.5 M Li_2SO_4 electrolyte (pH = 7): (a) 1st galvanostatic charge–discharge voltage profiles, (b) stability of specific discharge capacity, (c) coulombic efficiency, and (d) linear scan voltammetry for different current collectors in 2.5 M Li_2SO_4 (pH = 7) at a scan rate of 1 mV s^{-1}.

Another advantage of CCC aluminium is its capability to suppress undesired oxygen evolution at high charging potential as evidenced by cyclic voltammetry measurements.[31] As shown in Fig. 4(d), the oxygen evolution peak position varies with current collectors. Oxygen begins to evolve at the potentials of 1.1 and 1.7 V *vs.* Ag/AgCl on SS316 and untreated aluminium, respectively, while titanium and CCC aluminium push the values to 2.2 and 3.8 V *vs.* Ag/AgCl respectively. The oxygen evolution reaction involves multiple intermediate steps including formation of adsorbed intermediate species such as adsorbed O, OH, OOH.[32] The overpotential for oxygen evolution reaction arises from the reduction of relative stability and binding energies of these intermediate species on a given surface.[33] It has been shown that even a single monolayer of chromium(III) oxide on the CCC aluminium surface could effectively suppress the oxygen evolution reaction through blocking active adsorption sites and reducing the electron tunnelling rate.[34] This behavior contributes to the higher coulombic efficiency obtained from the electrodes fabricated on CCC aluminium foil (~99%) than those on SS316 mesh and untreated aluminium foil and similar to titanium foil in Fig. 4(c). In other words, oxygen evolution is suppressed before lithium is being extracted from $LiMn_2O_4$ during the charging process.

4. Conclusions

In summary, we demonstrated the effectiveness of chromate conversion coating on an aluminium foil current collector to achieve excellent corrosion-resistance in ALIB. Electrochemical measurements of $LiMn_2O_4$ electrodes fabricated on CCC aluminium showed superior capacity retention as well as higher coulombic efficiency than traditional stainless steel and titanium based current collectors. The CCC layer acts as (i) a physical barrier to aggressive ions and (ii) a reservoir of chromate ions which can diffuse to corrosion sites to form protective insoluble Cr(III) compounds, thereby enhancing the corrosion resistance of aluminium foil. We would like to point out that the chromate compounds used here are toxic and should be replaced by environmentally friendly materials going forward.[12] Nonetheless, we believe the excellent performance of CCC aluminium foil demonstrated here will spark interest in the development of lightweight low-cost current collectors to enable high energy density aqueous batteries.

Acknowledgements

The authors acknowledge the funding support from the Advanced Research Projects Agency-Energy (DE-AR0000380).

Notes and references

1 W. Li, W. R. Mckinnon and J. R. Dahn, *J. Electrochem. Soc.*, 1994, **141**, 2310–2316.
2 W. Tang, Y. Zhu, Y. Hou, L. Liu, Y. Wu, K. P. Loh, H. Zhang and K. Zhu, *Energy Environ. Sci.*, 2013, **6**, 2093–2104.

3 J.-Y. Luo, W.-J. Cui, P. He and Y. Y. Xia, *Nat. Chem.*, 2010, **2**, 760–765.
4 H. Kim, J. Hong, K. Y. Park, H. Kim, S. W. Kim and K. Kang, *Chem. Rev.*, 2014, **114**, 11788–11827.
5 S. Liu, S. H. Ye, C. Z. Li, G. L. Pan and X. P. Gao, *J. Electrochem. Soc.*, 2011, **158**, A1490–A1497.
6 H. Wang, Y. Zeng, K. Huang, S. Liu and L. Chen, *Electrochim. Acta*, 2007, **52**, 5102–5107.
7 M. Zhao, G. Huang, B. Zhang, F. Wang and X. Song, *J. Power Sources*, 2012, **211**, 202–207.
8 K. Xu and C. A. Angell, *J. Electrochem. Soc.*, 1998, **145**, L70–L72.
9 A. H. Whitehead and M. Schreiber, *J. Electrochem. Soc.*, 2005, **152**, A2105–A2113.
10 M. A. Elmorsi and R. M. Isaa, *Bull. Electrochem.*, 1988, **4**, 785.
11 R. P. Frankenthal and L. F. G. Mesias, Electronic materials, Components, and Devices, in *Uhlig's Corrosion Handbook*, John Wiley & Sons, Inc., Hoboken, NJ, USA, 3rd edn, 2011, pp. 559–564.
12 R. L. Twite and G. P. Bierwagan, *Prog. Org. Coat.*, 1998, **33**, 91–100.
13 J. Zhao, G. Frankel and R. L. McCreery, *J. Electrochem. Soc.*, 1998, **145**, 2258–2264.
14 MIL_5541_Specification "Chemical Conversion Coatings on Aluminium and Aluminium Alloys", 1990.
15 A. E. Hughes, R. J. Taylor and B. R. W. Hinton, *Surf. Interface Anal.*, 1997, **25**, 223–234.
16 Q. Meng and G. S. Frankel, *Surf. Interface Anal.*, 2004, **36**, 30–42.
17 L. E. M. Palomino, L. V. Aoki and H. G. deMelo, *Electrochim. Acta*, 2006, **51**, 5943–5953.
18 B. R. Strhmeier, *Surf. Interface Anal.*, 1990, **15**, 51–56.
19 G. P. Halada and C. R. Clayton, *J. Electrochem. Soc.*, 1991, **138**, 2921–2927.
20 M. U. Kendig, S. Jeanjaquet, R. Addison and J. Waldrop, *Surf. Coat. Technol.*, 2001, **140**, 58–66.
21 W. Tang, Y. Hou, F. Wang, L. Liu, Y. Wu and K. Zhu, *Nano Lett.*, 2013, **13**, 2036–2040.
22 J. M. Atebamba, J. Moskon, S. Pejovnik and M. Gaberscek, *J. Electrochem. Soc.*, 2010, **157**, A1218–A1228.
23 A. Sakuda, A. Hayashi and M. Tatsumisago, *J. Power Sources*, 2010, **195**, 599–603.
24 R. D. Armstrong and V. J. Braham, *Corros. Sci.*, 1996, **38**, 1463–1471.
25 G. M. Scamans, J. A. Hunter and N. J. H. Holroyd, 8th International Light Metals Congress, 1987, vol. 1, pp. 699–705.
26 G. M. Brown, K. Shimizu, K. Kobayashi, G. E. Thompson and G. C. Wood, *Corros. Sci.*, 1992, **33**, 1371–1385.
27 L. Xia and R. L. McCreery, *J. Electrochem. Soc.*, 1998, **145**, 3083–3089.
28 G. S. Frankel and R. L. Mccreery, *Electrochem. Soc. Interface*, 2001, **10**, 34–38.
29 D. Aurbach, M. D. Levi, K. Gamulski, B. Markovsky, G. Salitra, E. Levi, U. Heider, L. Heider and R. Oesten, *J. Power Sources*, 1999, **81–82**, 472–479.
30 G. Yuan, J. Bai, T. N. L. Doan and P. Chen, *Mater. Lett.*, 2014, **137**, 311–314.
31 G. J. Wang, N. H. Zhao, L. C. Yang, Y. P. Wu, H. Q. Wu and R. Holze, *Electrochim. Acta*, 2007, **52**, 4911–4915.
32 I. Katsounaros, S. Cherevko, A. R. Zeradjanin and K. J. J. Mayrhofer, *Angew. Chem., Int. Ed.*, 2014, **53**, 102–121.
33 R. V. Mom, J. Cheng, M. T. M. Koper and M. Sprik, *J. Phys. Chem. C*, 2014, **118**, 4095–4102.
34 W. J. Clark and R. L. Mccreery, *J. Electrochem. Soc.*, 2002, **149**, B379–B386.